Thin Solid Films 516 (2008) 8655–8662

Contents lists available at ScienceDirect

Thin Solid Films

journal homepage: www.elsevier.com/locate/tsf

Stress measurement in thin films with the ion beam layer removal method: Influence of experimental errors and parameters

S. Massl [a,*], H. Köstenbauer [a,b], J. Keckes [c], R. Pippan [a]

[a] Erich Schmid Institute of Materials Science, Austrian Academy of Sciences, A-8700 Leoben, Austria
[b] Department of Physical Metallurgy and Materials Testing, University of Leoben, A-8700 Leoben, Austria
[c] Department Materials Physics, University of Leoben, A-8700 Leoben, Austria

ARTICLE INFO

Article history:
Received 23 October 2007
Received in revised form 5 June 2008
Accepted 30 June 2008
Available online 6 July 2008

Keywords:
Ion beam layer removal method
Residual stresses
Thin films
Error analysis

ABSTRACT

A recently developed ion beam layer removal method allows the precise determination of complex depth profiles of residual stresses in crystalline and in amorphous thin films on a nanoscale [S. Massl, J. Keckes, R. Pippan, Acta Mater. 55 (2007) 4835]. Recipes and advice for optimal experimental design are given herein to minimize errors in the stress distributions calculated. The calculation procedure of this method is briefly introduced followed by the definition of any sources of error along with their influence on the resulting stress distribution. Finally, the errors as a function of experimental parameters are discussed by means of an example and four model stress distributions.

1. Introduction

Residual stresses and their distribution in thin films and structural elements in near-surface regions have been a field of intensive investigation because they are essential for the mechanical performance, the structural integrity and the lifetime of coated components. Such stresses are usually caused by thermal mismatch, the fabrication process or the applied load.

A number of methods have been developed for determining the average residual stresses in thin films. This is only useful when the residual stresses are distributed homogeneously. The mean stress is determined either directly by measuring the curvature of the coated system [1–3], or indirectly by calculating the film stress from the lattice strain determined by means of X-ray diffraction and the elastic constants of the film material [1,4]. Often, residual stresses are not distributed uniformly across the film thickness as a consequence of the growth process, thermal loading or the mechanical treatment. Such depth profiles can be determined by grazing incidence X-ray techniques [5], which achieve depth resolution on a nanoscale. However, these techniques can only be applied to crystalline materials and measure the stresses indirectly. Furthermore, the lateral resolution is limited to values > 100 μm owing to the grazing incidence of the X-rays and beam diameters of at least 1 μm.

Recently, a direct technique that allows the determination of complex depth profiles of residual stresses on a nanoscale called the ion beam layer removal method (ILR method), has been proposed [6]. It is based on the measuring of the deflection of a focused ion beam (FIB) workstation-fabricated micro cantilever beam as a function of the gradually reduced film thickness. This reproducible method can be applied to crystalline and amorphous materials.

Subsequently, ILR method is described briefly and the errors that influence the calculated stress distribution are then analyzed in detail. General guidelines for optimizing the experimental procedure are suggested and the advantages as well as limitations of the measures proposed for the minimization of errors are discussed.

2. Brief description of the ILR method

The ILR method allows the determination of depth profiles of residual stresses in crystalline and amorphous thin films. Such a residually stressed system induces a certain curvature depending on the stresses, the layer and substrate thicknesses, as well as the Young's moduli of the materials involved. Here, the ILR method is described with a 1.16 μm TiN film on a 450 μm thick (100)Si substrate. The thin film was deposited at 550 °C by means of reactive sputtering from a Ti target in an Ar + N_2 atmosphere using an unbalanced DC magnetron sputtering system. The ILR method is based on the fabrication of a micro cantilever beam of adequate dimensions in <010> direction of the Si in the vicinity of the specimen edge by means of a dual beam FIB which combines an ion column and a scanning electron microscope (SEM). This cantilever consists of the a few microns thick substrate and the thin film and deflects owing to the redistributed residual stresses. In the presented example depicted in Fig. 1, the cantilever deflects downwards due to the compressive stresses in the TiN film. In case of tensile stresses in the thin film, the cantilever would exhibit a

* Corresponding author. Tel.: +43 3842 804 214; fax: +43 3842 804 116.
E-mail address: stefan.massl@mu-leoben.at (S. Massl).

0040-6090/$ – see front matter © 2008 Elsevier B.V. All rights reserved.
doi:10.1016/j.tsf.2008.06.091

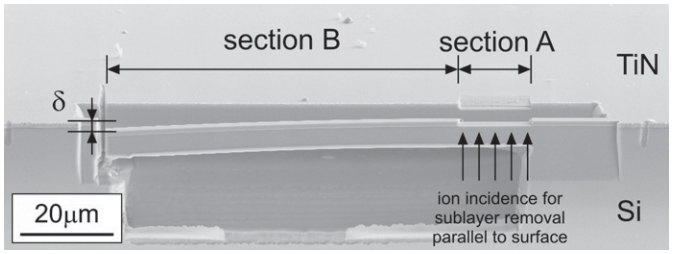

Fig. 1. Cantilever beam deflecting owing to compressive residual stresses in the thin film (inclined view). Then, the film is removed gradually in section A with the ion beam aligned parallel to the surface. This leads to a change of the curvature of section A amplified by section B, which acts as a curved indicator.

positive (upward) deflection. The deflection is measured from high magnification SEM images and corresponds to a certain curvature.

In order to measure the stress through the film, the thickness of the film thickness is reduced gradually from the top as with the ion beam aligned parallel to the sample surface as depicted in Fig. 1. The thin material slices removed from the film in each step are called sublayers and the thickness of the individual sublayers is determined from the difference of the film thicknesses between two consecutive steps. The rest of the cantilever, section B, still has the curvature of the original cantilever and acts as a curved indicator that amplifies the curvature of section A. The reduction of the film thickness in section A affects the stress state in this part, leads to a shift of the neutral axis and changes the deflection of the cantilever. The curvature of section A as a function of cantilever thickness is calculated from the corresponding actual deflection and the curvature of the initial cantilever. The deflection and curvature as a function of film thickness depicted in Fig. 2 is the basis for the calculation of the stress profile in the cantilever and the initial system.

The calculation procedure of the stress profile in the cantilever is based on the stepwise superposition of the previously removed sublayers in section A. To facilitate the evaluation procedure, the stresses of the actual straightened cantilever are used. This eliminates the contribution of the curvature to the stress profile and leads to homogeneously distributed stresses in the substrate as well as in each of the superimposed sublayers.

The calculation procedure for the first two steps is depicted schematically in Fig. 3. It starts with the uncoated substrate in section A, which is the last step of the of the sublayer removal procedure. At the beginning, the substrate is stress free and therefore straight as depicted in Fig. 3(1a). When the first sublayer is superimposed, it leads to a shift of the neutral plane. At this point, the sublayer is not subjected to residual stresses and has no influence on the stress distribution in the substrate

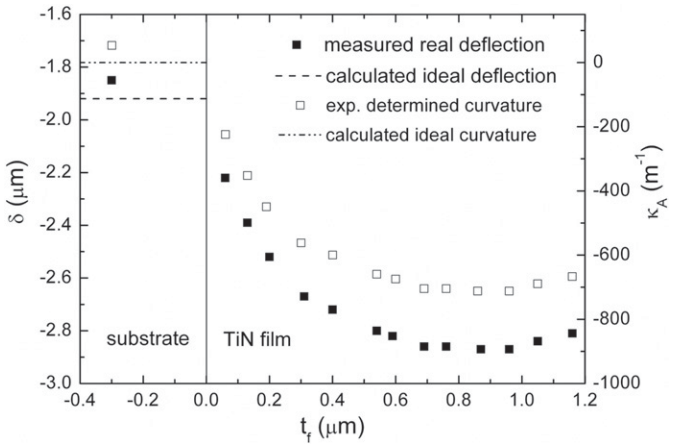

Fig. 2. Deflection of the cantilever obtained directly from SEM images and calculated curvature of section A as a function of the actual film thickness. For comparison, the deflection and curvature calculated for the completely removed thin film (t_f<0), which leads to a stress free straight cantilever in section A, is drawn in.

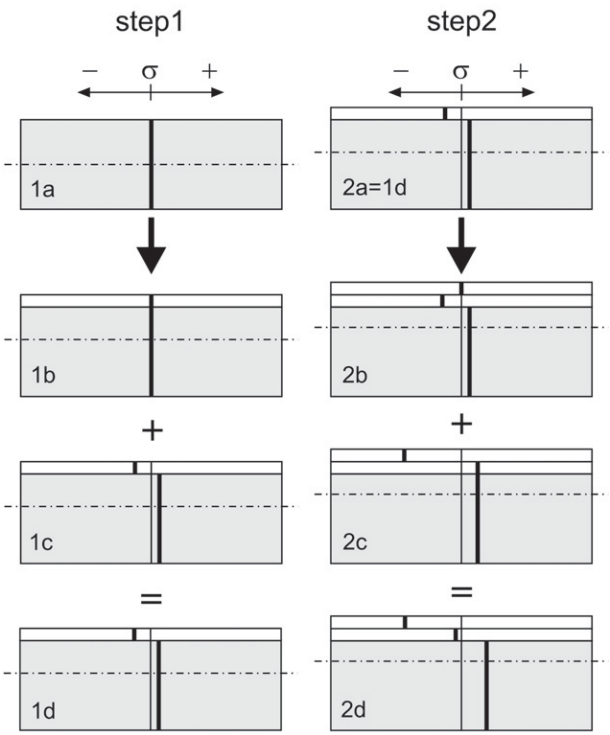

Fig. 3. The calculation procedure is described by means of the first two steps; each step starts with the balanced stress distribution of the previous step (a). Then, an unstressed sublayer is superimposed to obtain the composition of the current system (b). This leads to a shift of the neutral plane and a certain curvature. Now, an additional stress distribution (c) that consists of the stress in the superimposed sublayer and the corresponding balanced stress in the cantilever below is added. The stresses in (c) are chosen in such a way, that the addition of the stresses of (b) and (c) leads to the curvature and stress distribution of the current cantilever (d). The stress in each further sublayer superimposed is calculated in principle by the same procedure as applied in the second step.

below (Fig. 3(1b)). Now, system 1c is introduced. Having the same dimensions as system 1b, it is subjected to intrinsic residual stresses that consist of the stress in the sublayer and the corresponding balanced stress in the substrate. The magnitude of the residual stresses in 1c depends on the stresses in 1b and the curvature in 1d in a way that superimposing the systems 1b and 1c leads to the experimentally determined curvature of 1d. Step 2 starts with the system calculated in step 1d. The stress free sublayer 2 is superimposed, leading to a shift of the neutral axis as depicted in Fig. 2b. Then, system 2b is superimposed with system 2c, which is subjected to residual stresses in sublayer 2 and the corresponding balanced stresses in the system below consisting of the substrate and sublayer 1. As before, the superposition of 2b and 2c leads to the actual stress distribution 2d that results in the experimentally measured deflection or curvature, respectively.

The stress distribution in the initial cantilever is determined after superimposing the uppermost sublayer and completing the corresponding calculation procedure. The stress profile is described by a step function with step sizes corresponding to the thicknesses of the individual sublayers. Finally, the stress distribution in the initial system is calculated from the stress profile in the cantilever, since the stresses can be converted into each other as long as the materials involved exhibit linear elastic behaviour (Fig. 4).

Possible explanations for such a depth profile of residual stresses could be a gradient of defects or a change in the microstructure. For comparison, the film stress was determined by means of the conventional wafer curvature technique and Stoney's equation, which lead to a mean film stress of −1.21 GPa. This value is 21% smaller than the average stress obtained by means of the ILR method (−1.53 GPa) and is considered as a fairly good agreement. It has to be taken into account that the biaxial Young's moduli $E_b = E/(1-\upsilon)$ have to be used

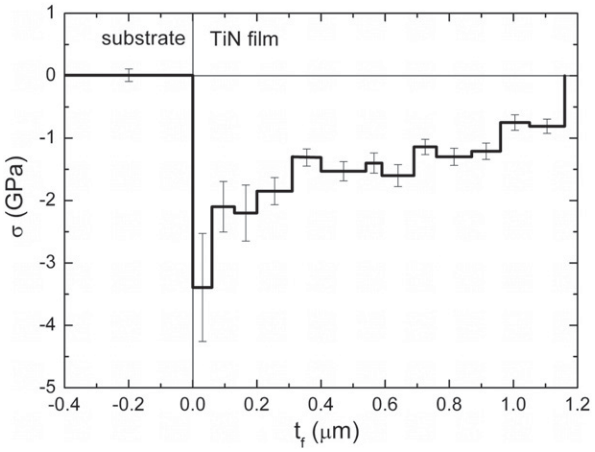

Fig. 4. Calculated stress distribution in the initial system. The thickness of each step of the step function corresponds to the thickness of the sublayers removed.

in the calculation procedure of the ILR method to consider the 2D calculation procedure of a 3D problem. In the presented example, the bulk Young's moduli and Poisson's ratios of Si ($E_{Si(100)}$=130 GPa±5%, ν_{Si}=0.28±0.01%) and TiN (E_{TiN}=309 GPa±24%, ν_{TiN}=0.27±14%) are taken from literature [7–22].

3. Discussion of sources of error

The stress distribution contains errors owing to ion damage, the finite accuracy in measuring the dimensions of the cantilever and the individual sublayers, the limited number of sublayers the thin film is divided into, as well as the uncertainty of the input material parameters. Additionally, an unfavourable choice of the cantilever thickness may lead to fracture or plastic relaxation of the layer or the substrate during the experiment which could lead to a wrong result and therefore has to be avoided. These sources of error and consequential general guidelines for a useful configuration of the experiment are discussed.

3.1. Ion damage

Ion damage cannot be avoided when working with a FIB. Implanted ions change the mechanical properties of the material as well as the residual stress field as shown by Kim et al. [23], and may therefore lead to notable errors.

The amount of ion damage generally depends on the ions and materials involved, the acceleration voltage, the incident angle and the ion current [24]. The penetration depth can be estimated by means of a simple SRIM (the stopping and range of ions in matter) [25] simulation which takes into account the parameters mentioned above. The estimations show that for many ion-material-combinations the implantation depth is between 10nm and 30nm. This is small compared to the typical thickness of the individual sublayers and therefore, the ion induced changes of the stress distribution can usually be neglected. This assumption was confirmed by experimental findings, where cantilevers of different materials and thicknesses were irradiated with Gallium ions under various angles of incidence and with different ion currents. Measuring the deflections prior and after this experiment showed no measurable changes which leads to the conclusion that the ion beam-induced stresses can be disregarded in the materials investigated. Anyway, it is advisable to perform a SRIM simulation prior to the experiment. Additionally, it is necessary to check the literature if the ions and materials involved lead to grain boundary embrittlement, as it is the case for Ga ions and Al, for example, since such effects are not considered in the SRIM software.

A simple way to minimize ion damage is to use low ion currents and low ion energies for fine FIB cuts and to check the diameter and shape of the ion beam prior to cutting, since in case of insufficient calibration or outworn FIB apertures the beam dimensions are usually not well defined.

3.2. Real and calculated stresses in a sublayer

The calculation procedure leads to a stress distribution in the thin film which is described by means of a step function as depicted in Fig. 4. As a result of the calculation procedure, the stresses in each of the individual sublayers are constant and can be approximated well by the mean stresses in each sublayer as long as the curvature is not too large. The quality of the reproduction of the real stress profile by the step function depends among others on the shape of the real stress profile and the thicknesses of the individual sublayers the film is divided into.

In case of a relatively homogeneous stress distribution, the subdivision of the film into a few relatively thick sublayers will reproduce the real stress profile well. In case of a rugged stress distribution, it is not possible to reproduce the details by means of a few thick sublayers. Rather, a large number of thin sublayers (~ 80nm) is favourable due to the increase in resolution of the stress profile. Nevertheless, it should be noted that the thickness of the individual sublayers can only be measured with finite accuracy. This leads to larger relative errors in thin sublayers and as a result to larger errors in the calculated sublayer stresses when thin sublayers are used. In other words, an increase of spatial resolution leads to an increase of errors of the stresses determined. This effect is explained in detail in Section 4 by means of four model stress distributions.

3.3. Accuracy of SEM measurements

The SEM-measured dimensions, such as cantilever lengths, thicknesses and deflections contain certain errors due to technical and physical limitations of the microscope, systematic errors owing to insufficient calibration and unavoidable statistical errors.

Technical and physical limitations of the SEM lead to a decrease in image quality with increasing magnification. Generally, such limitations cannot be compensated, but optimal settings for the acceleration voltage, stigmation, working distance, magnification and the choice of an adequate aperture ensure best image quality possible. Systematic errors which result from insufficient calibration, lead to a general over or underestimation of measured lengths. They are not easy to detect and statistical analysis is not generally useful to quantify such errors. Therefore, a careful calibration of the SEM prior to the experiment by means of a calibration device of defined length is essential. Statistical errors are fluctuations in observations which yield results that differ from measurement to measurement and that require repeated experimentation to obtain precise results [26]. Such errors of repeated independent measurements of the same length can generally be approximated well by the normal distribution. The statistical errors can be reduced significantly if the SEM is calibrated well, as demonstrated in case of the presented example, where the deflections are measured with a field emission SEM at a magnification of 20,000× with a standard deviation of only 10nm.

These errors in the measurements of the lengths of section A and B, l_A and l_B, the deflection δ, as well as the thicknesses of the cantilever substrate and the sublayers, $t_{sub,c}$ and t_{sl}, affect the determined stresses in a complex way. In order to get an idea of the most important parameters and to ensure a proper design of the experiment, the influence of the errors on four model stress distributions is discussed in Section 4.

3.4. Reliability of the values for the Young's moduli

The Young's moduli of the system have a great influence on the magnitude of the stresses determined because they affect the position of the neutral plane and associate the measured strains with the corresponding stresses according to the Hooke's Law. The Young's moduli used in the calculation procedure can be determined by means of one of the methods available [17–22]. Alternatively, elastic moduli

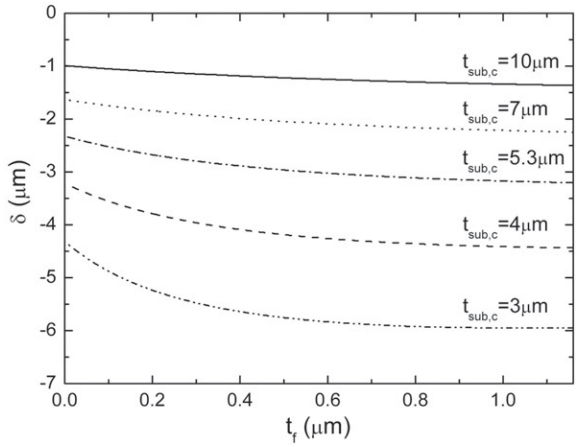

Fig. 5. Deflection of the cantilever as a function of film thickness calculated for various cantilever substrate thicknesses. The deflection is calculated for the 1.16 μm TiN film ($E_{b,TiN}$=400 GPa) on 450 μm Si substrate ($E_{b,Si(100)}$=180 GPa) and a mean film stress in the initial system of $\bar{\sigma}_f$=−1.21 GPa. The deflections calculated for a substrate thickness of 5.3 μm are similar to the measured deflections depicted in Fig. 2.

of the substrate and the thin film can be obtained from literature as it is the case in the presented example.

Depending on the materials and the testing procedure the values for the Young's moduli are more or less reliable. Especially for complex coating systems, it can be difficult to find useful values because the elastic properties depend strongly on the fabrication parameters which are often not well defined. Furthermore, the properties of the surface layer can be changed by the ion beam during the actual experiment. For most materials, usually only the first few nanometers are affected, which leads to the conclusion that the average Young's module of the thin film, and even the individual sublayers, is not shifted significantly. Often such errors have to be estimated because in many cases it is not possible to quantify them statistically. As with the errors of the SEM-measured dimensions, the influence of the errors of the Young's moduli will be investigated subsequently by means of four model stress distributions.

3.5. Fracture and plastic deformation

Fracture and plastic deformation of the substrate or the thin film has to be avoided during the experiment to ensure a linear elastic behaviour of the system. A simple way to prevent these effects is the choice of an adequate cantilever substrate thickness, which leads to convenient deflections and stresses which are significantly smaller than the fracture stress or the yield stress. Useful cantilever dimensions can be estimated by assuming a stress distribution probable for the investigated system and calculating the minimum and maximum stresses that occur during the experiment for various cantilever substrate thicknesses. A cantilever substrate thickness that gives reasonable deflections and presumably does not lead to fracture or plastic deformation is chosen as a suitable dimension for the actual experiment.

A reliable way to assure after the experiment performed that the calculated stress distribution is not influenced by plastic deformation or fracture is to compare the determined mean stresses of the ILR method to another method, for example the wafer curvature method. Possible fracture or plastification during the experiment would lead to a remarkable difference between the two mean stresses and would therefore indicate the invalidity of the experiment.

4. Experimental design to minimize errors in the stress distribution

The set-up as well as the actual experimental procedure can be optimized to minimize the errors mentioned above. Optimal cantilever dimensions to reduce the errors in the deflection measurement and to avoid fracture and plastic deformation are discussed along with comparing four model stress profiles with respect to the influence of the input errors like the SEM-measured dimensions and the Young's modulus of the film on the calculated result. The basic considerations and equations for the error analysis which is based on the Gaussian or normal error distribution are presented.

4.1. Useful choice of cantilever dimensions

Since the mean stress and the stress distribution is unknown during the planning of the experiments, an expected mean stress or an expected stress distribution should be used to estimate the deflection and the changes in the stress distribution during the cutting and removal procedure.

For the example presented, a mean film stress in the initial system of −1.21 GPa was determined by means of the wafer curvature method. The initial deflections are calculated for cantilevers with different substrate thicknesses, section lengths of l_A=16 μm and l_B=92 μm and the elastic moduli of the system presented. The film thickness in section A is reduced gradually and the actual deflections as a function of film thicknesses for selected substrate thicknesses as depicted in Fig. 5. In case of thick cantilevers, the deflection changes nearly linearly with the removed film thickness and the deflection and the change of the deflection is very small, which would complicate their exact measurement with the SEM. With decreasing substrate thickness, the initial deflections as well as the changes of the deflections increase and the shape of the curves become more nonlinear. On one hand, this makes the SEM readout of the deflections more accurate. However, large curvatures can result in plastic deformation or fracture of the involved structure or the substrate. Therefore, the dimensions of the cantilever have to be adjusted to the expected stresses, the thickness of the structure and the materials involved to avoid fracture or plastic deformation during the experiment and to achieve a convenient ratio between the error of the deflection measurement and the measured deflections $\Delta\delta/\delta$.

A useful initial deflection for a cantilever of 100 μm in length, for example, would be − 3.5 μm which corresponds to a curvature of − 700m^{-1}. After the stepwise removal of the entire thin film in section A (l_A=15 μm) a deflection of − 2.5 μm, which comes solely from the curved indicator, remains. Such initial and final deflections are a good choice for film thicknesses between a few hundred nanometers and a few micrometers because much larger deflections can lead to fracture or plasticity and smaller deflections contain large relative errors when measured with the SEM.

Cantilever substrate thicknesses that lead to such useful deflections can be obtained from Fig. 6 for various combinations of elastic moduli

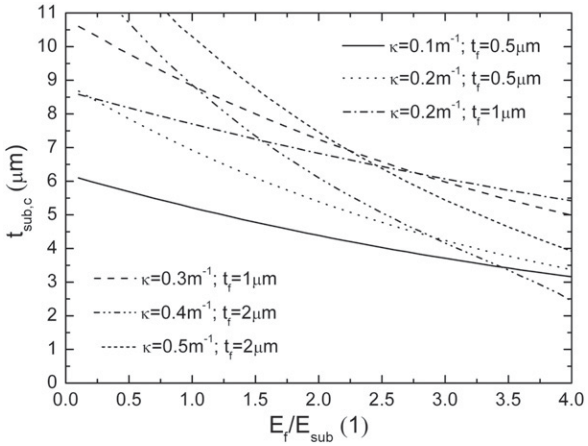

Fig. 6. Cantilever substrate thicknesses $t_{sub,c}$ that lead to initial deflections of −3.5 μm and final deflections of −2.5 μm as a function of the ratio E_f/E_{sub} for various combinations of curvature and film thickness of the initial system ($t_{sub,is}$=500 μm).

and film stresses. In order to include as many cases as possible, the film stresses are expressed by means of the constant curvatures of the initial systems. The curvature of this initial system has to be estimated or calculated from the film stress by means of Stoney's Eq. (1) [27].

$$\kappa = \frac{6\sigma_f t_f}{E_{b,sub} t_{sub,is}^2} \quad (1)$$

The estimations in Fig. 6 refer to initial systems of 500 μm substrate thickness. If the substrate of the initial system of interest is significantly thicker or thinner than 500 μm (anyway, $t_{sub,is} >> t_f$ has to be valid), the curves plotted in Fig. 6 cannot be used for the estimation. In this case, Eq.(2) which is derived from Stoney's equation is used to calculate the curvature of an initial system with the same film stress as the actual initial system but a substrate thickness of 500 μm.

$$\kappa_{500\,\mu m} = \frac{\kappa_x \cdot (t_{sub,x})^2}{(500\,\mu m)^2} \quad (2)$$

To estimate the tendency towards fracture and plastic deformation, the stresses in the curved cantilever as a function of film thickness should be analyzed. Nevertheless, it has to be kept in mind that this estimation is based on the assumed mean stress or stress distribution in the thin film of the initial system and that it can differ significantly from the real stress distribution, which would lead to different variation of the stresses during the experiment.

Another relevant point is the choice of the lengths of section A, from which the film is removed stepwise, and section B, the indicator that amplifies the curvature.

Generally, section B should be as long as possible to amplify the deflection changes of section A efficiently. This length does not influence the occurrence of plastic deformation or fracture, since the stresses in the cantilever only depend on the substrate thickness. However, large dimensions lead to long milling times, therefore lengths of section B between 50 μm and 100 μm have proven to be a good compromise between amplification of the curvature of section A and FIB milling time.

In principle, section A should be as large as possible to produce a pronounced change of curvature when a sublayer is removed, but it is not possible to remove curved sublayers with the FIB, especially when we take into account that the curvature changes during the removal of the film. Therefore, straight sublayers are removed and the length of section A has to be limited in order to neglect the curvature, which assures nearly constant film thickness in section A at each step and facilitates the calculation procedure. For a typical curvature of the cantilever of about $700 m^{-1}$, a length of section A of approximately 15 μm leads to useful curvature changes and well defined sublayer geometries.

The cantilever width does not influence the calculation of the stress distribution as long as it is larger than the film thickness. Therefore, it does not contribute directly to the calculation of errors. The cantilever should not be wider than a few microns because imperfect parallel alignment of the ion beam and the film surface leads to wedge-shaped sublayers and the thickness of the sublayers cannot be measured correctly. The error in thickness measurement increases with increasing cantilever width. This relatively weak effect is not included explicitly in the following calculation of errors and can be considered in the input error for the thickness measurement.

4.2. Description of the four model stress distributions used for the error analysis

Four model stress distributions in layered structures on thick substrates are compared to investigate the influence of the experimental parameters and the input errors on the stress profile determined by means of the ILR method. These depth profiles of residual stresses depicted in Fig. 7 are chosen to show that the effect of the input errors on the calculated result depends significantly on the type of stress distributions investigated. For simplification, all four layered structures are 1.2 μm thick, the biaxial Young's moduli of the four films are $E_{b,f}$=400 GPa, and the biaxial moduli of the 500 μm thick substrates are $E_{b,sub}$=200 GPa. Stress profile (a) called "e-function" represents a distribution where the tensile stresses grow exponentially from 1 GPa at the surface to 2 GPa at the interface. (b) is a simple homogeneous stress profile with 1 GPa tensile stress. (c) describes a stress distribution with a constant gradient ranging from −1 GPa at the interface to 1 GPa at the surface. (d) represents a square wave signal-type stress profile where the stress alternates between 1 GPa and 2 GPa with a "wavelength" of 600nm. The average stresses in the initial systems lie between 0 GPa in case of the stress profile with the constant gradient as depicted in Fig. 7(c) and 1.5 GPa in case of the square wave signal-type stress distribution in Fig. 7(d).

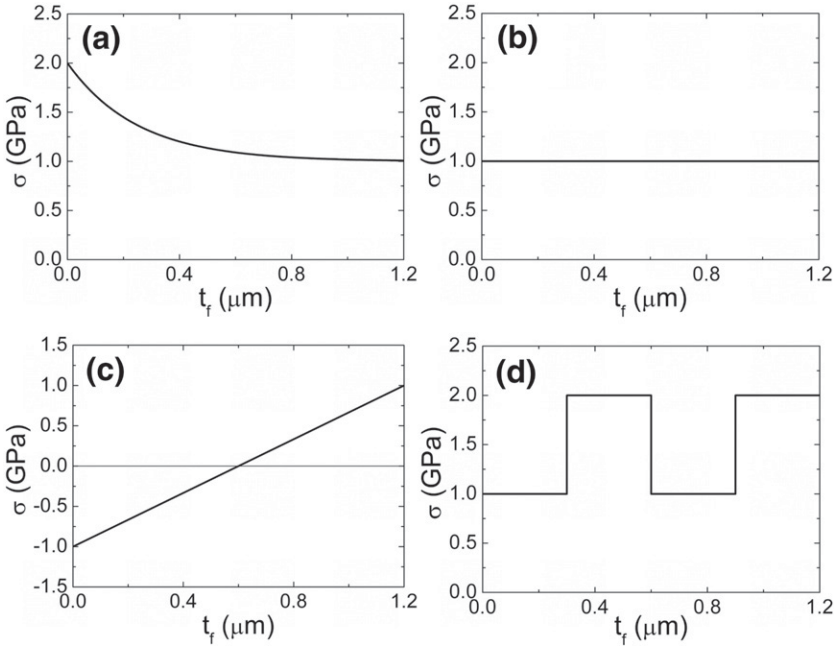

Fig. 7. Four model stress distributions in thin films on thick substrates represent basic types of stress profiles: (a) e-function, (b) homogeneous, (c) gradient and (d) stress variation.

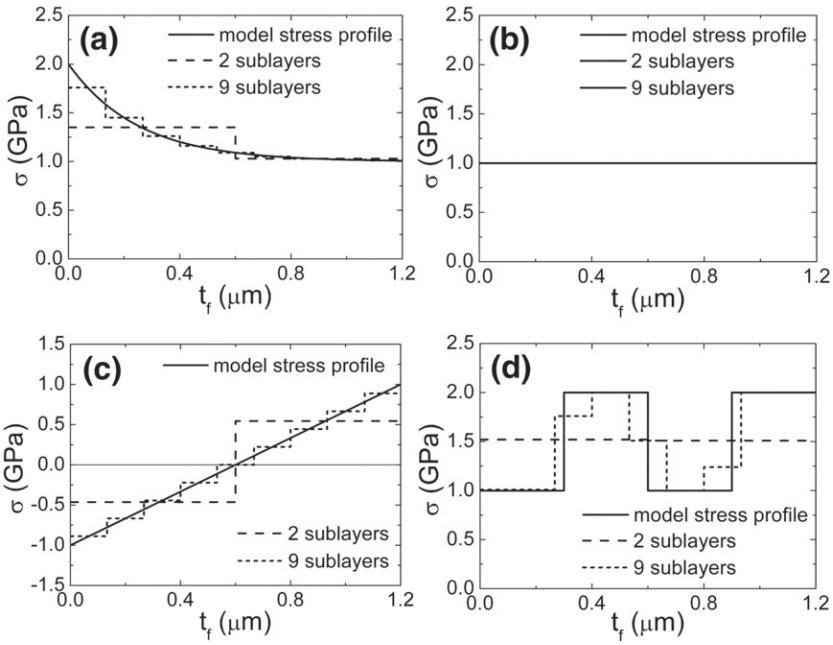

Fig. 8. Description of the four model stress distributions by means of the ILR method. Here, each thin film is divided into 2 and 9 sublayers, which leads to a more or less good approximation of the real depth profile of residual stresses.

4.3. Description of the error analysis

The measured dimensions and deflections as well as the values for the Young's moduli are described by Gaussian or normal distributions. This is physically useful because the normal distribution describes the distribution of random observations for most experiments [26]. It furthermore serves as approximation for the literature values of the Young's moduli. Thus, the magnitude of the input errors is described by the corresponding standard deviations, provide useful data and allow the use of simple calculations to determine the propagation of errors. For example, if a deflection δ contains the error $\Delta\delta$, 68% of the repeatedly measured values of this deflection are within $\delta \pm \Delta\delta$.

The propagation of the input errors and the resulting error of the stress profile is described by Eq.(3) which describes the dependence of the error of the stress distribution $\Delta\sigma$ on the stress σ itself, the input variable x_i and the corresponding standard deviation Δx_i of the input variable. Eq.(3) considers the phenomenon that errors cancel each other out partially [26].

$$\Delta\sigma = \sqrt{\sum_{i=1}^{n}\left(\frac{\partial\sigma}{\partial x_i}\Delta x_i\right)^2} \tag{3}$$

4.4. Influence of sublayer thickness, deflection and Young's modulus

In this section, the influence of the sublayer thickness and deflection measurement as well the Young's modulus of the film on the errors of the stresses determined is analyzed and discussed. Concerning the sublayer thickness measurement, we have to distinguish between two types of errors:

1. the quality of the reproduction of the real stress distribution
2. the effect of the sublayer thickness on the error of the stress distribution determined.

First, a high number of thin sublayers are required to approximate complicated stress distributions by the corresponding step function as detailed as possible. Thin sublayers are especially important when a jagged stress profile is expected. The correlation parameter C that quantifies the degree of approximation of the real stress distribution $f(t)$ and the approximated step function $g(t)$ is calculated from Eq.(4). A small correlation parameter corresponds to a good approximation and vice versa.

$$C = \frac{\sqrt{\int (f(t)-g(t))^2 \mathrm{d}t}}{\sqrt{\int f(t)^2 \mathrm{d}t}} \tag{4}$$

The four model stress distributions, each approximated by two step functions with two and nine sublayers, respectively, are depicted in Fig. 8. The dependence of the correlation parameter C on the number of sublayers i is demonstrated for each of these four model stress distributions in Fig. 9. As expected, the approximation of (a) and (c) improves with a growing number of sublayers, whereas the homogeneous stress profile (b) is approximated well for any number of sublayers. In case of the stress variation profile (d), the correlation is best when the number of sublayers is a multiple of the number of stress variations.

Secondly, an increase in the number of sublayers leads to a decrease in the mean sublayer thickness and therefore to larger relative errors in the thickness measurement. Therefore, an increase of the

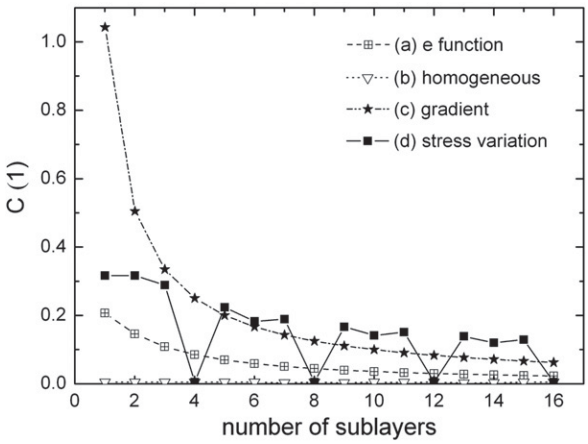

Fig. 9. Correlation parameter C as a function of the number of sublayers the films are divided in.

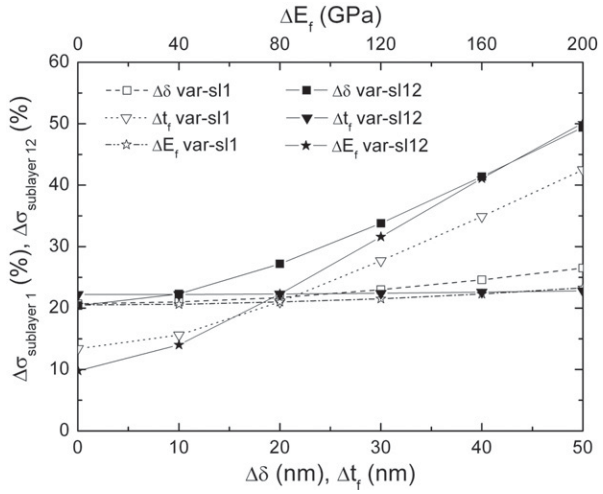

Fig. 10. The standard deviation $\Delta\sigma$ of the calculated stress in the undermost sublayer 1 (open symbols) and uppermost sublayer 12 (full symbols) of the stress profile depicted in Fig. 7(b). While one of the three parameters increases, the other two are kept constant at the values listed in Table 1.

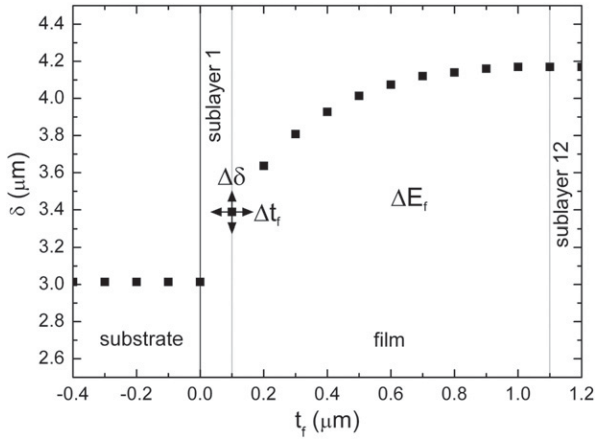

Fig. 11. Illustration of the errors $\Delta\delta$, Δt_f, ΔE_f in the measured deflection versus film thickness-function.

error of the calculated stresses is expected when the error of the thickness measurement increases.

A detailed error analysis of the homogeneous model stress distribution (the thin film in Fig. 7(b) is divided into 12 sublayers) is performed to investigate the influence of the error of the sublayer thickness measurement on the error of the resulting stress profile. The effect of the deflection measurement and the film's Young's modulus are examined. To ensure useful information, sublayer 1 (at the interface) and sublayer 12 (at the surface) are analyzed. Fig. 10. shows that the influence of the three parameters ($\Delta\delta$, Δt_f, ΔE_f) on the error of the stress distribution depends on the position of the investigated sublayer. While the accuracy of the measurement of the sublayer thickness is essential for small errors in sublayer 1, exact measurement of the deflection and a good choice of the film's Young's modulus ensure small errors in sublayer 12. This behaviour can be explained by analyzing the deflection as a function of film thickness for the homogeneous stress distribution and the influence of the three errors on this curve depicted in Fig. 11. The influence of the three errors on the sublayer stress deviation depends on the position of the sublayer and the corresponding local gradient of the deflection function.

The error in sublayer 1, which is located next to the substrate, depends mostly on the accuracy of the sublayer thickness measurement because a small variation of the sublayer thickness leads to large changes in the deflection due to the large gradient in the function. The deflection measurement leads to a moderate increase of the standard deviation of the stress calculated, which can also be explained by means of the strong gradient of the curve. The error in the Young's modulus of the film does not have a great influence because the substrate thickness is large compared to the current film thickness.

The error in the uppermost sublayer, sublayer 12, shows a different behaviour: The accuracy of the sublayer thickness measurement does not lead to large errors because the weak gradient of the deflection function leads to hardly any change in the corresponding deflection. On the other hand, the deflection measurement itself is very important for small errors. A small error in the film's Young's modulus is essential because the error in the modulus influences the position of the neutral plane as well as the actual calculation procedure significantly. This effect is especially pronounced when only few sublayers of the film were removed and the film thickness is not thin compared to the cantilever substrate thickness.

Table 1
Input values and input errors used for the error analysis

t_{sub} (μm)	t_f (μm)	$t_{sublayer}$ (nm)	$E_{sub,b}$ (GPa)	$E_{f,b}$ (GPa)	l_a (μm)	l_b (μm)
3	1.2	100	200	400	15	85
Δt_{sub} (nm)	Δt_f (nm)	$\Delta\delta$ (nm)	$\Delta E_{sub,b}$ (GPa)	$\Delta E_{f,b}$ (GPa)	Δl_a (nm)	Δl_b (nm)
150	20	10	20	80	200	300

5. Determination of Young's moduli of thin films

As already mentioned, the ILR method needs the knowledge of the Young's moduli for the determination of the residual stress distribution. However, with some additional information the ILR method can be used to calculate the Young's modulus of thin films when the mean stress in the film is known, for example, by means of the wafer curvature method. Therefore, first the mean stress in the thin film is determined from the curvature of the sample by means of Stoney's equation [27], which is independent of the Young's modulus of the thin film. Then, the stress profile in the thin film is calculated by means of the ILR method, which requires the thin film's modulus. The average stresses determined by means of the two methods are compared and the film's modulus of the ILR method is varied. The actual Young's modulus of the thin film is found when both mean stresses are equal.

Another possibility is the fabrication of cantilevers of significantly different substrate thicknesses. Then, the elastic modulus of the film can be determined by finding the Young's modulus that fits best the resulting variations in the displacements.

6. Final remarks and guidelines

Depending on the stress distribution, an appropriate choice of the number of sublayers can reduce the error of the correlation parameter C and therefore the total error of the ILR method dramatically. Especially for complex stress distributions, a large number of thin sublayers is a good choice because the details of rugged stress profiles can be reproduced well. In case of homogeneous stress distributions, a small number of thick sublayers can lead to more accurate results. However, a homogeneous stress distribution usually cannot be assumed prior to the experiment, therefore the division of the thin film into many thin sublayers is the most important measure for obtaining accurate results.

The cantilever dimensions – especially the substrate thicknesses – have to be adjusted to the estimated mean stresses to obtain useful deflections and to avoid plastic deformation or fracture during the experiment. Since the optimal substrate thickness depends on the film thickness, the materials involved and the stress distribution, general

simple advice about the optimal thickness cannot be given. Therefore, the best way is to estimate the resulting changes of the deflection for an estimated stress distribution. The cantilever length is a compromise between short FIB milling times, pronounced deflections and homogenous film thicknesses in section A during the reduction of the film thickness. Lengths of section B around 90 μm and of section A of about 15 μm have proved to be a good choice.

The accuracy of the sublayer thickness and deflection measurement as well as the Young's modulus/moduli of the layered structure influence the errors in the stress profile calculated significantly. The analysis of the errors in individual sublayers of a homogeneous model stress distribution shows that the influence of these three parameters depends strongly on the position of the sublayers and the corresponding local gradient of the deflection as a function of film thickness.

Acknowledgements

The authors thank the Austrian Science Foundation FWF for supporting this work and I.C. Noyan, C. Brand, K.J. Martinschitz and M. Cordill for their helpful discussions.

References

[1] E. Eiper, K.J. Martinschitz, J. Keckes, Powder Diffr. 21 (2006) 25.
[2] D. Resnik, U. Aljancic, D. Vrtacnik, M. Mozek, S. Amon, Vacuum 80 (2005) 236.
[3] T. Dieing, B.F. Usher, Phys. Rev. B 67 (2003) 054108.
[4] I.C. Noyan, J.B. Cohen, Residual Stress, Springer, New York, 1987.
[5] C. Genzel, Mater. Sci. Technol. 21 (2005) 10.
[6] S. Massl, J. Keckes, R. Pippan, Acta Mater. 55 (2007) 4835.
[7] L.B. Freund, S. Suresh, Thin Film Materials, Cambridge University Press, Cambridge, 2003, p. 244.
[8] C. Mendibide, P. Steyer, C. Esnouf, P. Goudenau, D. Thiaudiere, M. Gailhanou, J. Fontane, Surf. Coat. Technol. 200 (2005) 165.
[9] T. Kitamura, H. Hirakata, T. Itsuji, Eng. Fract. Mech. 70 (2003) 2089.
[10] J. An, Q.Y. Zhang, Surf. Coat. Technol. 200 (2005) 2451.
[11] H.C. Barshilia, B. Deepthi, A.S.A. Prabhu, K.S. Rajam, Surf. Coat. Technol. 201 (2006) 329.
[12] S.W. Bedell, A. Reznicek, K. Fogel, J. Ott, D.K. Sadana, Mater. Sci. Semicon. Process. 9 (2006) 423.
[13] G. Carlotti, L. Doucet, M. Dupeux, Thin Solid Films 296 (1997) 102.
[14] Z. Novotna, R. Kralova, R. Novak, J. Marek, Surf. Coat. Technol. 116–119 (1999) 424.
[15] J.D. Comins, W. Pang, A.G. Every, D. Pietersen, Refract. Met. Hard Mater. 16 (1998) 389.
[16] J. Haider, M. Rahman, B. Corcoran, M.S.J. Hashmi, Mater. Proc. Technol. 168 (2005) 36.
[17] M.J. Bamber, K.E. Cooke, A.B. Mann, B. Derby, Thin Solid Films 398–399 (2001) 299.
[18] S.-H. Kim, Mater. Lett. 61 (2007) 3589.
[19] Z. Huang, G. Leighton, R. Wright, F. Duval, H.C. Chung, P. Kirby, R.W. Whatmore, Sens. Actuators A 135 (2007) 660.
[20] J. Zhang, J. Mater. Process. Technol. 123 (2002) 329.
[21] J.M. Antunes, J.V. Fernandes, N.A. Sakharova, M.C. Oliveira, L.F. Menezes, Int. J. Solids Struct. 44 (2007) 8313.
[22] M.D. Tran, J. Poublan, J.H. Dautzenberg, Thin Solid Films 308–309 (1997) 310.
[23] Y.-R. Kim, P. Chen, M.J. Aziz, D. Branton, J.J. Vlassak, J. Appl. Phys. 100 (2006) 104322.
[24] D. Kiener, C. Motz, M. Rester, M. Jenko, G. Dehm, Mater. Sci. Eng. A 459 (2007) 262.
[25] J.F. Ziegler, J.P. Biersack, U. Littmark, The Stopping Range of Ions in Matter, Pergamon Press, New York, 1985, p. 321.
[26] P.R. Devington, Data Reduction and Error Analysis for the Physical Sciences, Mc Graw-Hill Book Company, New York, 1991.
[27] W.D. Nix, Metall. Trans. A 20A (1989) 2217.